JOURNAL OF CATALYSIS 33, 457–473 (1974)

Crystallite Size Effects in the Low-Temperature Oxidation of Ammonia Over Supported Platinum

J. J. OSTERMAIER,* J. R. KATZER AND W. H. MANOGUE†

Department of Chemical Engineering, University of Delaware, Newark, Delaware 19711

Received October 2, 1973

The effect of crystallite size on the specific catalytic activity of supported platinum catalysts in ammonia oxidation with molecular oxygen was determined. Rates of ammonia oxidation were measured in a differential, fixed bed, flow reactor between 393 and 473°K, and catalysts containing average crystallite sizes of 2.0, 2.7 and 15.5 nm (1 nm = 10 Å) were used. Nitrogen and nitrous oxide were the only nitrogen-containing products with about four times as much nitrogen as nitrous oxide. The initial specific catalytic activity of the large crystallite catalyst was higher than the 2.0 and 2.7 nm catalyst by factors of 5.7 and 3.7, respectively. All catalysts showed a marked decline in activity in the first 6 hr of operation with steady-state activity being reached in about 12 hr. Smaller crystallites were more severely deactivated so that the resultant steady-state specific activity of the large crystallite catalyst was greater by factors of 14 and 8. Both the specific catalytic activity and the selectivity, also a function of crystallite size, are explained in terms of the changes in average surface concentration of active oxygen with changes in crystallite size. The reaction rate data are best represented by a Langmuir-Hinshelwood model involving dissociative adsorption of both reactants.

NOMENCLATURE

D	degree of dispersion of metal
K_i	adsorption parameter in Langmuir-Hinshelwood kinetic model for species i, atm^{-1}
K'_i	equilibrium constant for surface reaction i
k_s	surface reaction rate constant in Langmuir-Hinshelwood kinetic model, s^{-1}
k_i	rate constant for surface reaction step i
P_i	partial pressure of species i, atm
r_i	rate of reaction with respect to species i as turnover number, s^{-1}
θ_i	fraction of surface covered by species i

Subscripts

I	initial
ss	steady state
vs	vacant site

INTRODUCTION

The effect of crystallite size in the range of 1.0 to 15.0 nm on the specific catalytic activity of supported metal catalysts has received much attention recently. Most of it has focused on hydrocarbon reactions over platinum and nickel under a reducing environment. Specific catalytic activity in hydrogenation reactions (*1–5*), dehydrogenation of cyclohexane (*6*, *7*) and methylcyclopentane (*8*), isomerization and dehydrocyclization of hexanes (*9*), isomerization of neopentane (*10*), and hydrogenolysis of cyclopentane (*3*, *4*) is generally independent

* Present address: Davison Chemical Co., Division of W. R. Grace, Washington Research Center, Clarksville, Maryland.

† Experimental Station, E. I. duPont de Nemours and Co., Wilmington, Delaware.

of metal crystallite size. These reactions have been called facile (*2*, *11*). Specific catalytic activity in neopentane cracking (*10*), isomerization of methylcyclopentane (*12*), deuterium exchange with benzene (*5*) and dehydrocyclization of *n*-heptane (*7*) has been shown dependent on platinum crystallite size, and these reactions have been referred to as demanding (*2*, *11*).

Much less work has been reported for reactions carried out under an oxidizing environment. Boreskov and co-workers (*13*, *14*) observed no crystallite size effect in the oxidation of SO_2 and H_2 over supported platinum but worked only with catalysts containing platinum crystallites which were larger than 5.0 nm, a range where such an effect would not be expected (*4*). Andersen, Green and Steele (*15*) reported that in the oxidation of pollutants over a platinum catalyst performance is different under oxidizing than under reducing conditions. Platinum in a very highly dispersed state has been observed to have a markedly lower activity after contact with oxygen in hydrogenation (*2*) and in fuel cell applications (*16*). Poltorak and co-workers (*3*,*4*) have shown significant changes in specific catalytic activity with crystallite size for several oxidation reactions over the same Pt/SiO_2 catalysts used for their hydrogenation studies (*3*, *4*, *17*, *18*). The specific catalytic activity for ethanol oxidation, for example, is two orders of magnitude lower over a catalyst with a platinum dispersion of 0.95 than over one with a dispersion of about 0.45 and is approximately the same on platinum black, which has a very low degree of dispersion, as on the less highly dispersed supported catalyst. Wilson and Hall (*19*) and Freel (*20*) have shown that oxygen chemisorption stoichiometry on supported platinum depends on crystallite size and pretreatment conditions.

Previous work in our laboratory has shown that the oxidation of ammonia by oxygen over supported platinum in an integral reactor between 473 and 573°K exhibits a marked crystallite size effect in the ratio of nitrogen to nitrous oxide produced (*21*). At lower temperatures oxidation reactions exhibit a deactivation which is highly dependent on the reaction conditions (*22*).

This work examined the effect of changing platinum crystallite size from 2.0 to 15.5 nm on specific catalytic activity and selectivity in the oxidation of ammonia with molecular oxygen between 393 and 473°K.

Experimental Details

Apparatus

A packed bed, continuous flow, microreactor was used to obtain the data. Conversion of limiting reactant was always below 10%, and differential operation was confirmed by demonstrating that reaction rate was independent of space velocity in the range of operation. A manifold system containing rotameters and flow controllers was used to measure and mix oxygen and ammonia (either pure or premixed in helium) with helium to give the desired feed composition. The reactor and preheat coil were immersed in a fluidized sand bath (±1°K); a thermocouple in the catalyst bed demonstrated equality of bath and reactor temperature. A bypass loop allowed the reactor to be isolated from the system. Exit gas from the reactor passed through two gas sample values used to inject samples into an F & M Model 810 dual-column gas chromatograph, so that the instantaneous rate of reaction could be measured as a function of time on stream. All lines were 316 stainless steel, and the reactor consisted of ¼ in. tubing between two Swagelok unions containing 250 mesh stainless screen. Helium was passed over a heated reduced copper oxide catalyst (Harshaw No. Cu-803-1/8) and then a 4A molecular sieve to remove oxygen and water.

Platinum metal surface area of catalysts was measured by hydrogen chemisorption, oxygen chemisorption, and hydrogen–oxygen titration using a constant volume static sorption apparatus similar to that of Joyner (*23*). Hydrogen and helium were cleaned by passage through a 5A molecular sieve trap at liquid nitrogen temperature. X-Ray line broadening measurements were made with a General Electric X-ray diffractom-

eter. Crystallite size determination from the above information was standard (*24*, *25*).

Materials

Gases. All gases were from Matheson Chemical Co. Helium was high purity, and mixed gases were 6% NH_3 and 25% high purity O_2, respectively, in high purity helium. Mixed gases contained <25 ppm N_2. Oxygen was high purity (99.99%), and hydrogen used for chemisorption was ultrahigh purity (99.999%).

Catalysts. Three different catalysts were prepared and studied. Harshaw alumina (Al-0104 Lot No. 30, initially as 3.2 mm pellets) was crushed and screened, and the 30–40 mesh range material was retained. This was washed to remove fines, dried for 24 hr at 398°K and then calcined in air at 973°K for 12 hr to stabilize the support. The catalysts were prepared by impregnating the alumina with a solution containing sufficient $Pt(NH_3)_4(OH)_2$ to give the desired metal content and evaporating the water at 343°K for 36 hr. The catalysts containing 1.0 and 2.93 wt% Pt were dried for a further 12 hr at 373°K under vacuum and at 393°K under air, respectively.

Catalyst reduction involved first contacting with flowing hydrogen at room temperature for 1 hr and then heating under flowing hydrogen as follows. For the 1% Pt catalyst the temperature was raised at 1°K/min to 623°K where it was held for 18 hr; the 2.93% Pt catalyst was heated at 2°K/min to 673°K for 6 hr. A portion of the 1% Pt catalyst was sintered in air at 923°K for 24 hr to increase the platinum crystallite size. This catalyst was then reduced in flowing hydrogen at 773°K for 12 hr.

The catalysts were characterized by hydrogen chemisorption, oxygen chemisorption, and hydrogen–oxygen titration. Catalysts were rereduced in the chemisorption apparatus at 623°K for 12 hr under flowing hydrogen and evacuated at $<10^{-6}$ Torr for 10 hr before making chemisorption measurements. The stoichiometry variations of Wilson and Hall (*19*) and Freel (*20*) were observed. For example, the unsintered 1% Pt catalyst, which had experienced only mild reduction conditions, had ratios of 1.5:1.0:3.9 for hydrogen chemisorption: oxygen chemisorption: hydrogen–oxygen titration; whereas after sintering the ratios were 1.2:1.0:3.0. Crystallite sizes were calculated from hydrogen chemisorption results (*24*) for all catalysts except the sintered 1% Pt catalyst where the hydrogen–oxygen titration results were used because of the low platinum surface area for this catalyst. An assumed 1:1 Pt_s–O stoichiometry was used in accord with Wilson and Hall (*19*) because of the large crystallite size. Table 1 summarizes the results.

X-Ray diffraction traces of the unsintered catalysts were the same as that of the alumina indicating the absence of crystallites greater than ~3.0 nm. Debye line broadening for the sintered 1% Pt catalyst indicated a volume average crystallite size of 21.0 nm—in essential agreement with the chemisorption results. Electron micrographs of the unsintered 1% Pt catalyst indicated that essentially all of the platinum crystallites fall between 2.0 and 3.0 nm. Essentially all of the platinum crystallites for the sintered 1% Pt catalyst fall between 8.0 and 20.0 nm with a volume average diameter of 14.0 nm calculated from 50 particles (*24*).

TABLE 1
CHEMISORPTION CHARACTERIZATION OF SUPPORTED PLATINUM CATALYSIS

Catalyst	(g moles H_2 adsorbed/g catalyst)[a] × 10^6	Platinum dispersion	Surface av crystallite size[b] (nm)
2.93% Pt	38.4	0.52	2.0
Unsintered 1% Pt	9.83	0.38	2.7
Sintered 1% Pt	1.71	0.065	15.5[c]

[a] Gram moles of surface platinum atoms per gram of catalyst is twice hydrogen chemisorption per gram.

[b] Calculated as the edge length of a cube with five sides exposed from hydrogen chemisorption data (*24*).

[c] From hydrogen–oxygen titration.

Procedure

The catalysts underwent marked deactivation in the first 2 hr, reaching steady-state activity in about 6 hr. Since performance was dependent on deactivation conditions and on previous reaction history, a standard deactivation and run procedure was followed. Each catalyst was deactivated at the operating temperature in an oxygen-rich environment to prevent time dependent changes in the steady-state activity with changing gas-phase composition, and a 1% NH_3 and 5% O_2 in helium stream was used in all cases. Although steady-state activity was reached in less than 12 hr, in all cases 18 hr were allowed before steady-state kinetic data were taken.

When it was desired to measure steady-state activity at less than 10% conversion, the amount of catalyst charged to the reactor was typically 1.4, 6.5, and 6.5 g for runs at 433, 413 and 393°K. Resulting space velocities were typically 5.8, 1.3 and 0.55 s^{-1}. At the start of a run the entire system was purged with high purity helium for 20 min, and the total flow and feed composition were set using the reactor bypass. Feed was diverted over the catalyst, and periodic activity measurements were begun after about 5 min. Kinetic data were obtained for oxygen concentrations of 1–5% and for ammonia concentrations of 0.5–5% in helium. Pressure was atmospheric. Because the reaction is highly exothermic with about a 130°K adiabatic temperature rise per 1% ammonia consumed, temperatures, ammonia concentrations and conversions were kept low to avoid significant deviations from isothermality. The oxygen concentration range was scanned at each of four ammonia concentrations. Whenever the flow was to be diverted from the reactor, the reactor was first purged with an oxygen-rich feed because a static, ammonia-rich atmosphere reactivated the catalyst.

Initial rate data were obtained separately at 1% NH_3 and 3% O_2, and appropriately higher space velocities to keep conversion below 10%. The effluent nitrogen and nitrous oxide concentration was followed at 5 min intervals for 35 min.

The exit gas stream from the reactor was analyzed for N_2, N_2O and O_2. N_2 and O_2 were separated on a 2 m 5A molecular sieve column; N_2O on a 3 m Chromosorb 104 column both at 40°C.

Rates are reported as turnover numbers which are defined as the number of gram moles of ammonia reacted per gram mole of surface platinum atoms per second. For nitrogen and nitrous oxide formation, rates are in terms of gram moles of nitrogen or nitrous oxide per gram mole surface sites. Each surface site was assumed to consist of two surface platinum atoms, where the number of surface platinum atoms was determined by hydrogen chemisorption.

Results

Site of Catalytic Activity

No reaction was observed when a feed of 1% NH_3 and 1% O_2 in helium was passed over the alumina support at 473°K showing that catalysis is associated with the platinum. A correlation between platinum surface area as measured by hydrogen chemisorption and the observed rate of reaction is indicated in Table 2. Increasing the platinum loading from 1.0 to 2.93% resulted in a 3.9-fold increase in metal surface area and a 2.1-fold increase in the observed rate of reaction. If a significant fraction of the observed reaction were occurring on the support as a result of reactant spillover from the platinum surface, a much poorer correlation between observed rate and metal surface area should exist. The difference from direct proportionality is due to a difference in crystallite size for the two catalysts which is shown below to affect the activity per unit metal surface area.

TABLE 2
Relation of Observed Rate to Platinum Surface Area

Catalyst	Pt metal surface area/g catalyst, as g moles H_2 chemisorbed/g	Rate[a] (g moles NH_3/g cat-hr)
Unsintered 1% Pt, 2.7 nm	9.83×10^{-6}	1.1×10^{-4}
2.93% Pt, 2 nm	38.4×10^{-6}	2.3×10^{-4}

[a] Conditions: 413°K, 1% NH_3, 3% O_2 in helium.

Effect of Crystallite Size on Specific Catalytic Activity

The initial specific catalytic activity [turnover number (s^{-1})] was obtained by plotting the natural logarithm of the rate obtained in the initial rate studies against time on stream and extrapolating the resulting smooth curve to zero time. The estimates are believed accurate to within ±20% of the true value. Figure 1 is a typical deactivation curve for the unsintered 1% Pt catalyst at 393°K.

The effect of temperature on initial specific catalytic activity of the three catalysts

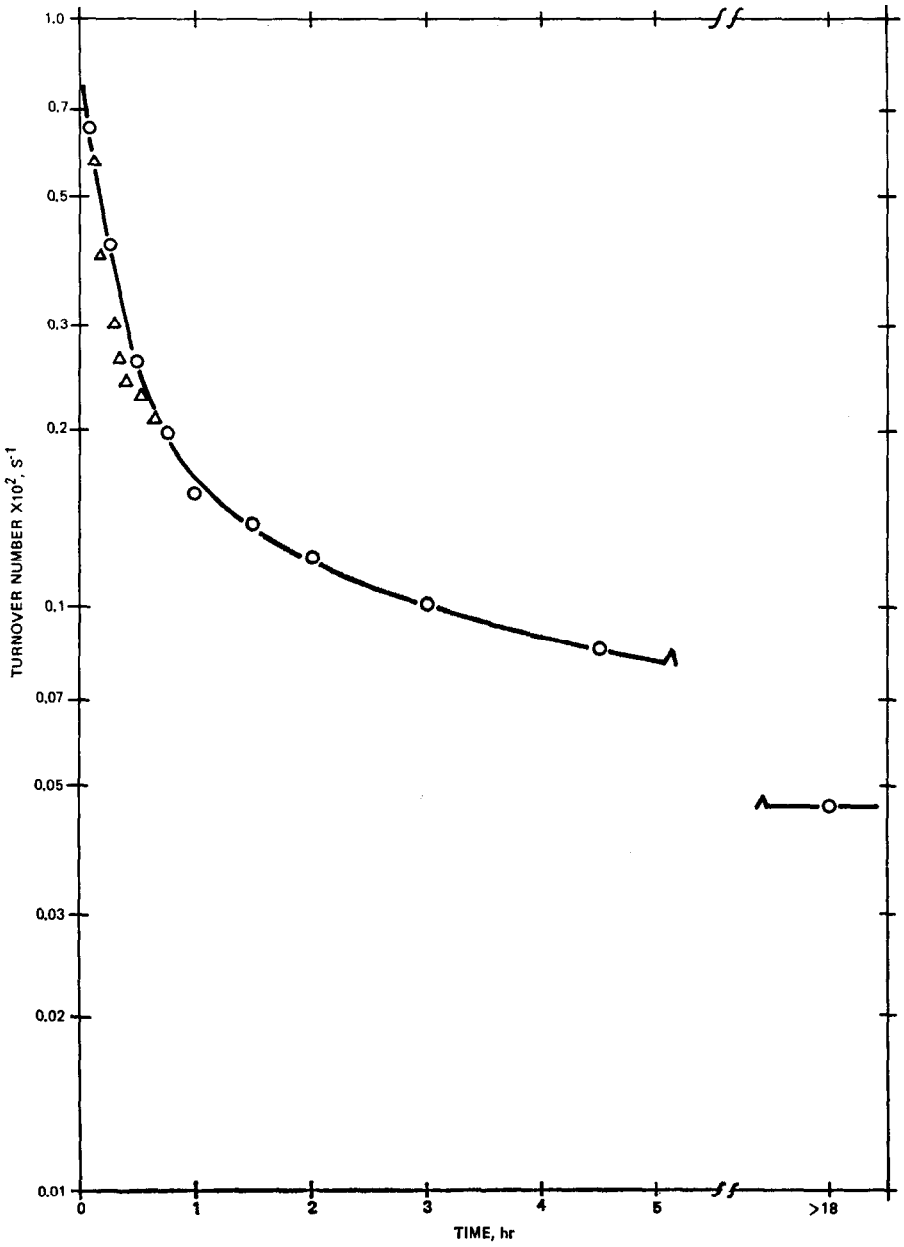

FIG. 1. Deactivation to steady state of unsintered 1% Pt catalyst at 393°K: (○) conditions used for obtaining steady-state kinetic data; (△) conditions used in obtaining initial rate data; 1% NH_3 and 3% O_2 in helium, both deactivations.

studied for a feed of 3% O_2 and 1% NH_3 is shown in Fig. 2. The sintered 1% Pt catalyst (15.5 nm) is 3.7 times more active per surface platinum atom than the unsintered 1% Pt catalyst (2.7 nm), and the ratio is independent of temperature. The sintered 1% Pt catalyst is 5.5 times more active than that of the 2.93% Pt catalyst (2.0 nm). The observed Arrhenius activation energy for the rate over the two 1% Pt catalysts is 9 ± 2 kcal/mole.

Figure 3 shows the steady-state specific catalytic activity of the three catalysts as a function of platinum crystallite size and temperature for the same feed composition used in Fig. 2. Values are the average of

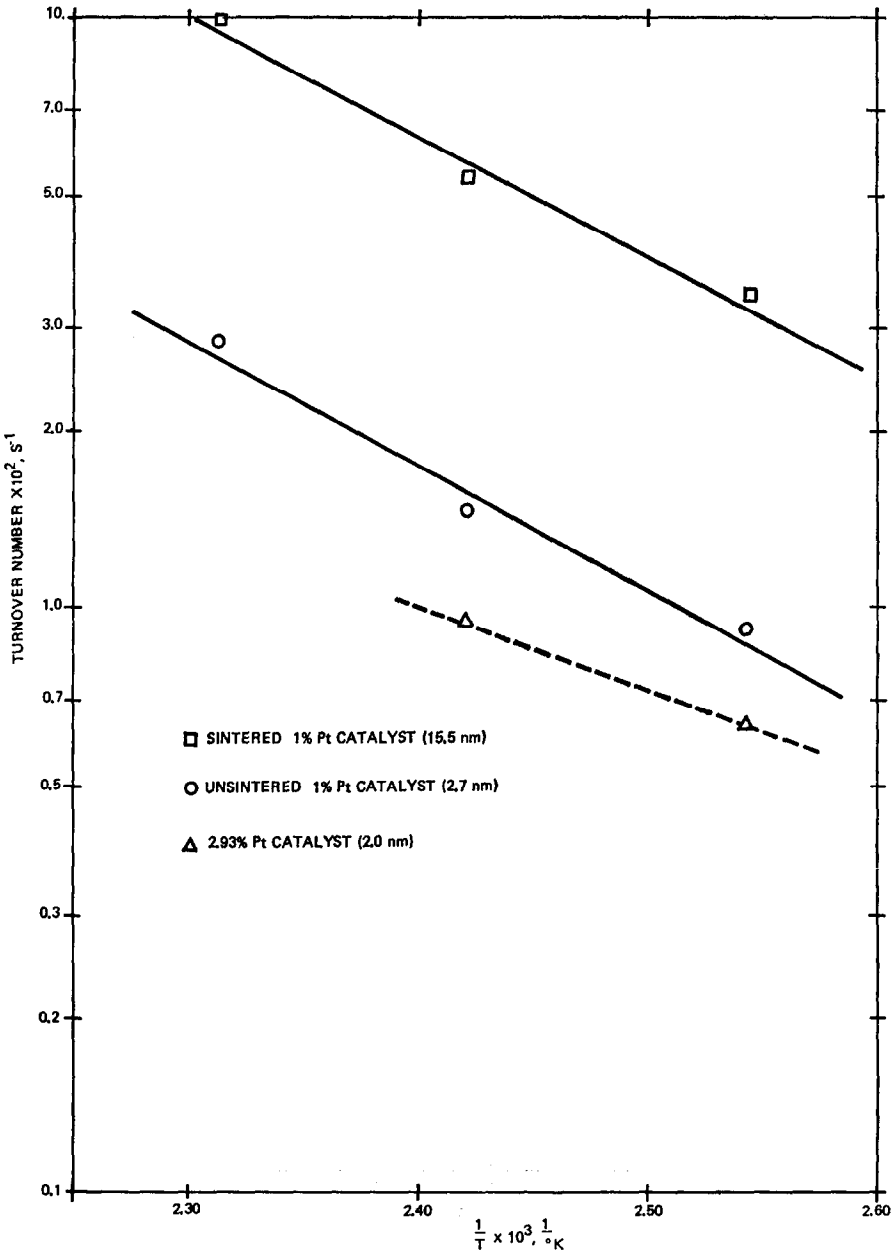

FIG. 2. Dependence of initial specific catalytic activity for ammonia oxidation on temperature and catalyst.

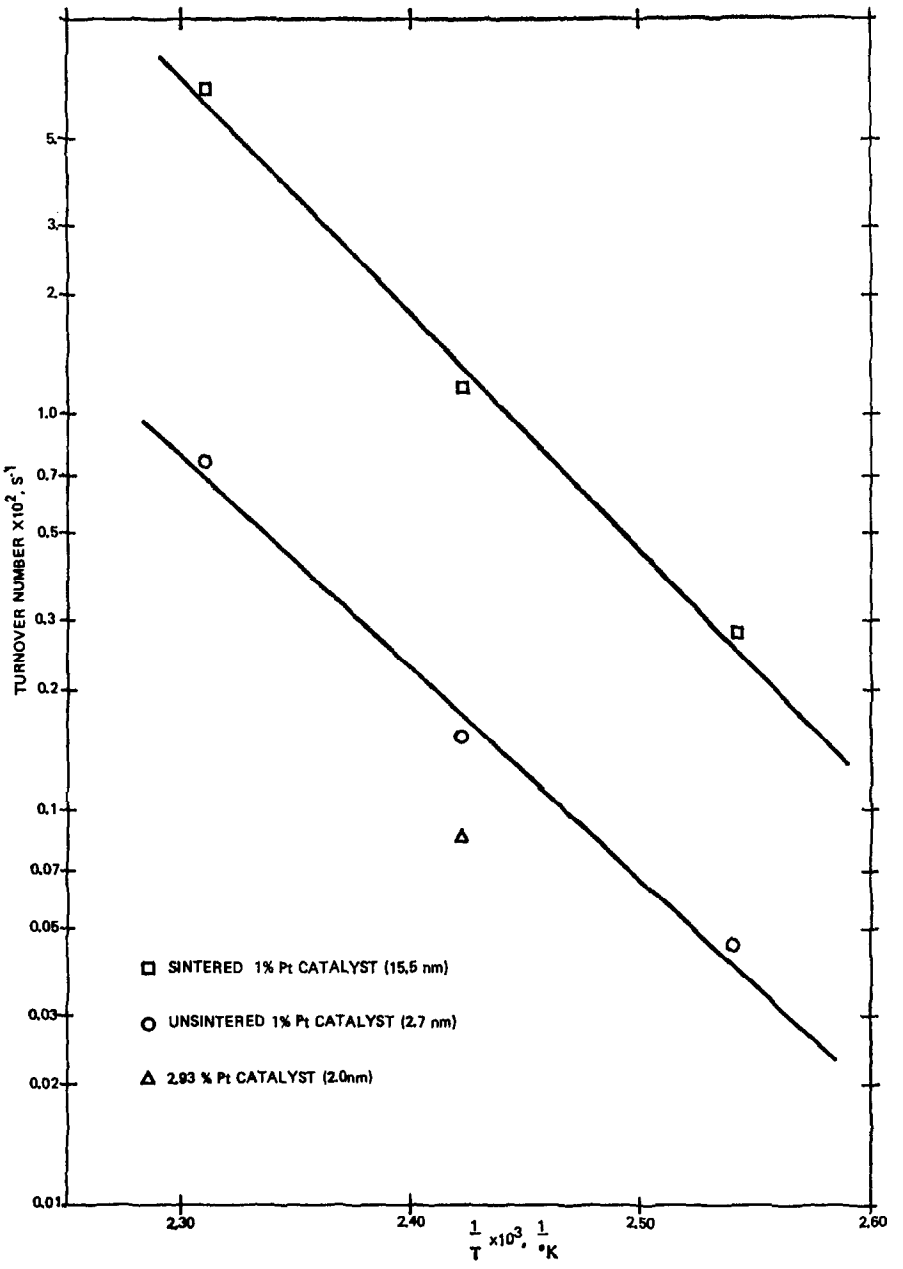

FIG. 3. Temperature dependence of steady-state specific catalytic activity.

several runs and are better than ±10%. The specific catalytic activity of the sintered 1% Pt catalyst again is higher than that of the unsintered 1% Pt catalyst but in this case the ratio is temperature dependent. It is 6.6 at 393, 7.8 at 413 and 8.8 at 433°K. At 413°K the specific catalytic activity of the sintered 1% Pt catalyst is 14 times that of the 2.93% Pt catalyst. The Arrhenius activation energies are 24 and 27 ± 2 kcal/mole for the 2.7 and 15.5 nm crystallite catalysts. The specific catalytic activity appears to curve upward with increasing temperature rather than obey strictly linear Arrhenius behavior. It was not possible to deactivate the catalyst at

TABLE 3
EFFECT OF CRYSTALLITE SIZE AND TEMPERATURE ON EXTENT OF DEACTIVATION

Temp (°K)	Catalyst	r_I/r_{ss}[a]
393	Unsintered 1% Pt	22
	Sintered 1% Pt	12
413	2.93% Pt, 2.0 nm	12
	Unsintered 1% Pt, 2.7 nm	9.9
	Sintered 1% Pt, 15.5 nm	4.5
433	Unsintered 1% Pt	4.1
	Sintered 1% Pt	1.6

[a] Feed: 1% NH_3, 3% O_2, r_I = initial rate, r_{ss} = steady-state rate.

453°K because the reaction usually lit-off and under these conditions deactivation was not observed (*21*, *22*).

Table 3 gives the ratio of the initial specific catalytic activity to that at steady-state as a function of both temperature and platinum crystallite size. The extent of deactivation for the unsintered 1% Pt catalyst is twice that of the sintered 1% Pt catalyst, and the ratio is essentially independent of temperature although the extent of deactivation for both crystallite sizes decreases by a factor of 5 between 393 and 433°K. The 2.93% Pt catalyst exhibits even greater deactivation confirming that the extent of deactivation is crystallite size dependent.

Effect of Crystallite Size on Selectivity

The only products of reaction observed at temperatures below 200°C were N_2, N_2O and H_2O; NO was not detected. This is in accord with DeLaney and Manogue (*21*). Table 4 shows that selectivity to nitrogen increases with decreasing platinum crystallite size and is independent of temperature. Deactivation to steady-state activity increases the selectivity by about 25% with highly dispersed platinum (Fig. 4) but does not affect the selectivity with the 15.5 nm crystallite catalyst (Table 4). Steady-state nitrogen production is about 50% greater per mole of ammonia reacted over the 2.7 nm crystallite catalyst than over the 15.5 nm crystallite catalyst.

The dependence of selectivity at partial conversion on feed composition is shown in Fig. 5 for 413°K. In all cases the selectivity to nitrogen increases as the ammonia partial pressure is increased and as the oxygen partial pressure is reduced (P_{NH_3}/P_{O_2} increases) although the selectivity is only weakly dependent on oxygen and ammonia partial pressures.

Table 5 summarizes the selectivity to nitrogen for a feed gas and bath temperature of 473°K. Under this condition light-off occurs due to particle instability, and conversion of the limiting reactant is essentially 100% at the same space velocity

TABLE 4
EFFECT OF CRYSTALLITE SIZE ON PRODUCT SELECTIVITY

Temp (°K)	Catalyst	$\left(\frac{r_{N_2}}{r_{N_2O}}\right)_I^a$	$\left(\frac{r_{N_2}}{r_{N_2O}}\right)_{ss}^a$
393	2.93% Pt, 2.0 nm	3.6	—
	Unsintered 1% Pt, 2.7 nm	3.6	4.6
	Sintered 1% Pt, 15.5 nm	3.1	2.7
413	2.93% Pt	3.9	4.9
	Unsintered 1% Pt	3.5	4.2
	Sintered 1% Pt	3.0	3.0
433	Unsintered 1% Pt	3.6	4.5
	Sintered 1% Pt	2.8	3.0

[a] Feed: 1% NH_3, 3% O_2, I refers to initial rates, ss refers to steady-state rates.

TABLE 5
SELECTIVITY TO NITROGEN AT 100% CONVERSION OF LIMITING REACTANT AND 473°K FEED WITH LIGHT-OFF

Catalyst	Reactant concn (%) NH_3	O_2	r_{N_2}/r_{N_2O}
Unsintered 1% Pt, 2.7 nm	1	1	10
Sintered 1% Pt, 15.5 nm	1	0.5	41
Sintered 1% Pt	1	1	16
Sintered 1% Pt	1	3	4.6
Unsintered 0.5% Pt[a], 4.3 nm	1	3	1.25
Sintered 0.5% Pt[a], 45 nm	1	3	3.0

[a] Data from DeLaney and Manogue (*21*), for commercial Pt/Al_2O_3 catalyst. Platinum crystallite size increased by sintering in air for 17 hr at 1053°K.

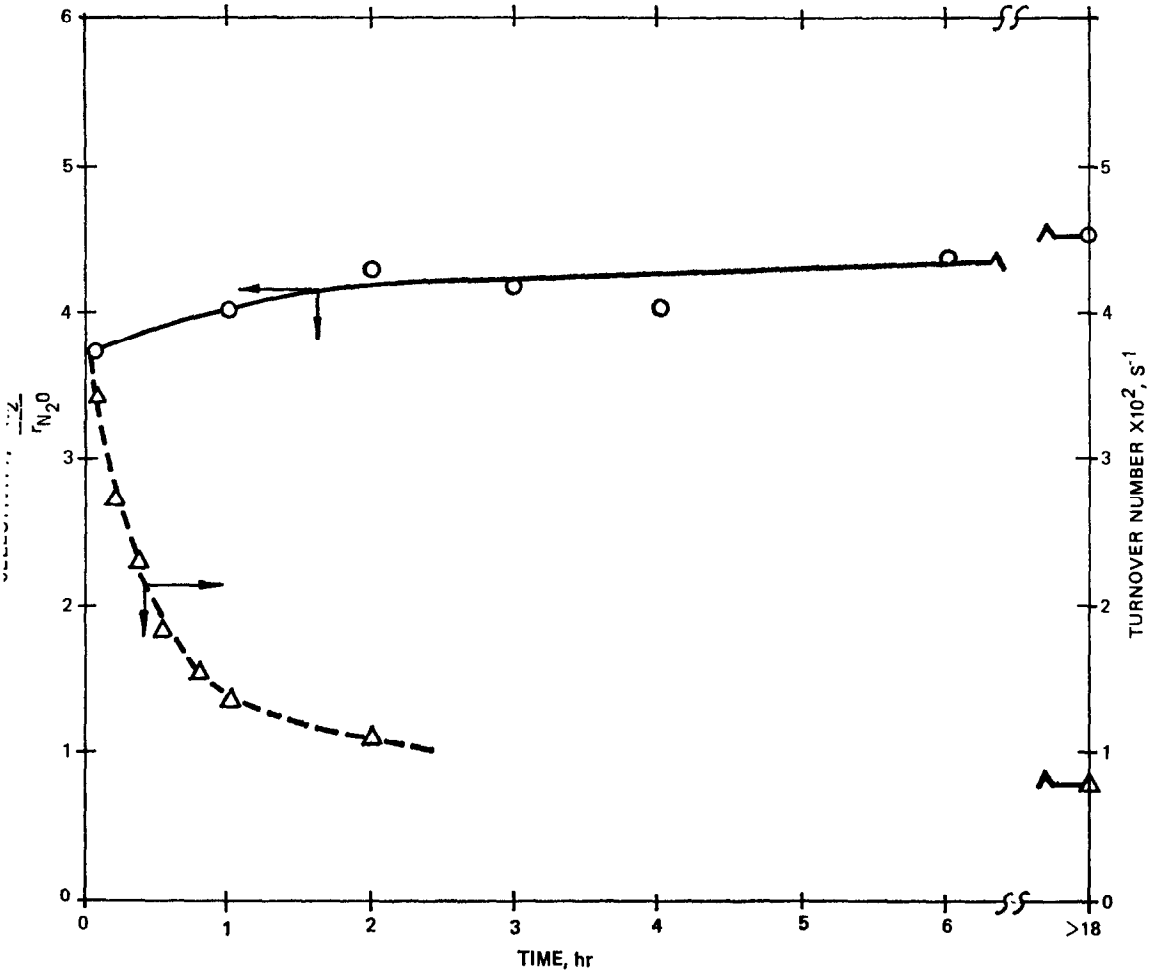

FIG. 4. Dependence of nitrogen selectivity on deactivation of unsintered 1% Pt catalyst at 433°K: (○) selectivity; (△) activity; Feed: 5% O_2, 1% NH_3, remainder helium.

as the 433°K studies. The last two entries in Table 5 are from DeLaney and Manogue (*21*) for 3.2 mm pellets of a commercial 0.5% Pt/Al_2O_3 catalyst. The platinum of their unsintered catalyst was amorphous to X-ray, and hydrogen chemisorption measurements indicated a surface average crystallite size of 4.3 nm (*26*). Platinum crystallites in their sintered catalyst were about 45 nm (*21*). Both sets of results show that platinum crystallite size affects the selectivity to nitrogen, larger crystallites giving higher nitrogen yields. The differences in selectivity that exist between the two studies are undoubtedly due to differences in study conditions. The nitrogen selectivity decreases as oxygen partial pressure is increased at temperatures both above (Table 5) and below (Fig. 5) 453°K. For temperatures above 453°K the selectivity is more strongly dependent on oxygen partial pressure. For the higher temperature condition the trend in selectivity with crystallite size is opposite that for the lower temperature, partial oxidation conditions.

Rate Models

The NH_3–O_2 kinetic data were fit to several Langmuir-Hinshelwood kinetic models using a standard nonlinear, least squares fitting technique. Models tested were single-site models involving the four possible per-

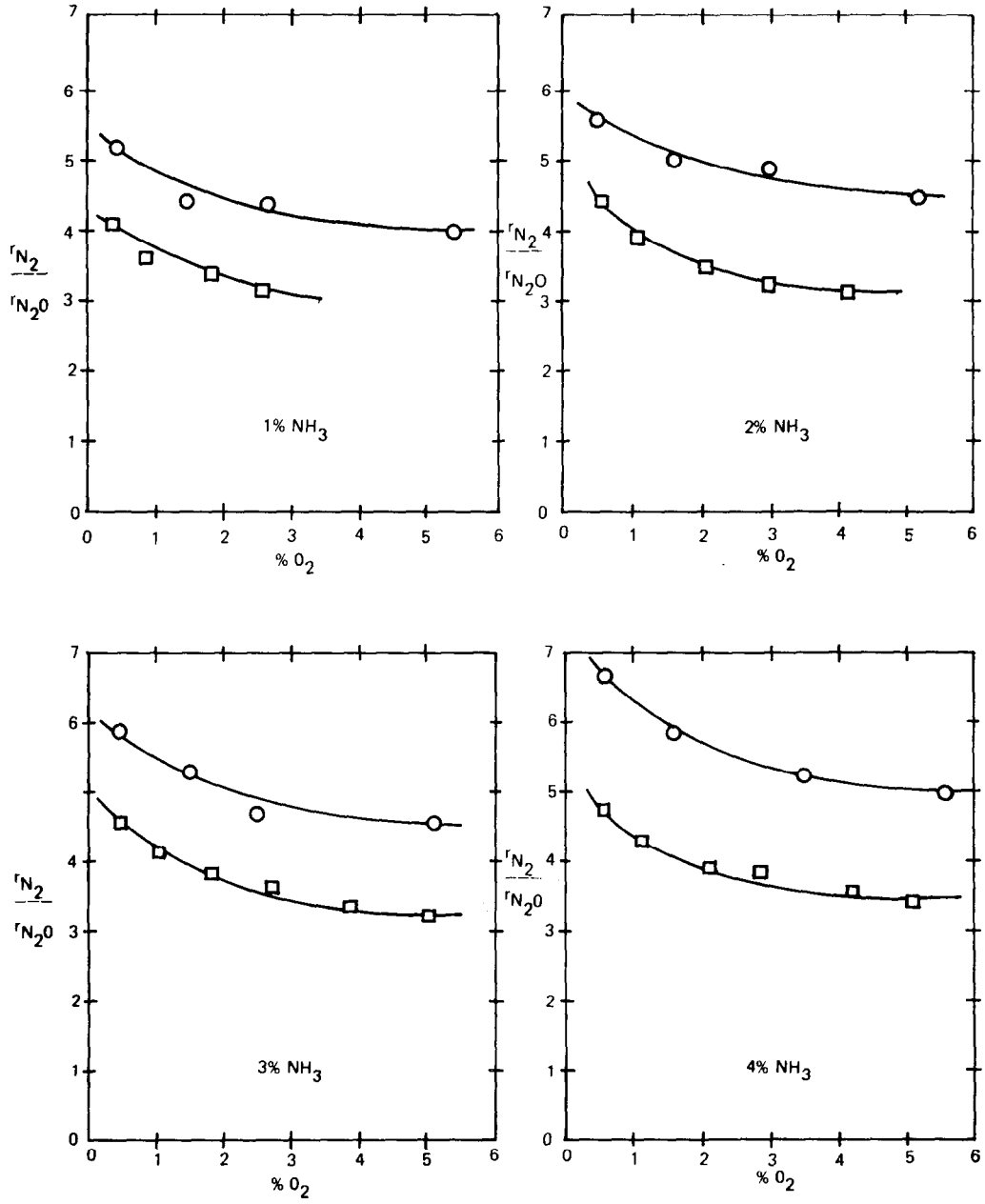

FIG. 5. Dependence of nitrogen selectivity on feed composition at 413°K: (○) unsintered 1% Pt catalyst; (□) sintered 1% Pt catalyst.

mutations of nondissociative and dissociative adsorption of ammonia and oxygen (*27*). Other models, for example models involving adsorption of either reactant as rate limiting or Rideal-type mechanisms, were considered but not tested because they did not correctly represent the observed dependence of the reaction rate on reactant concentration.

Both models involving the nondissociative adsorption of oxygen represented the data poorly as shown by the broken curves in

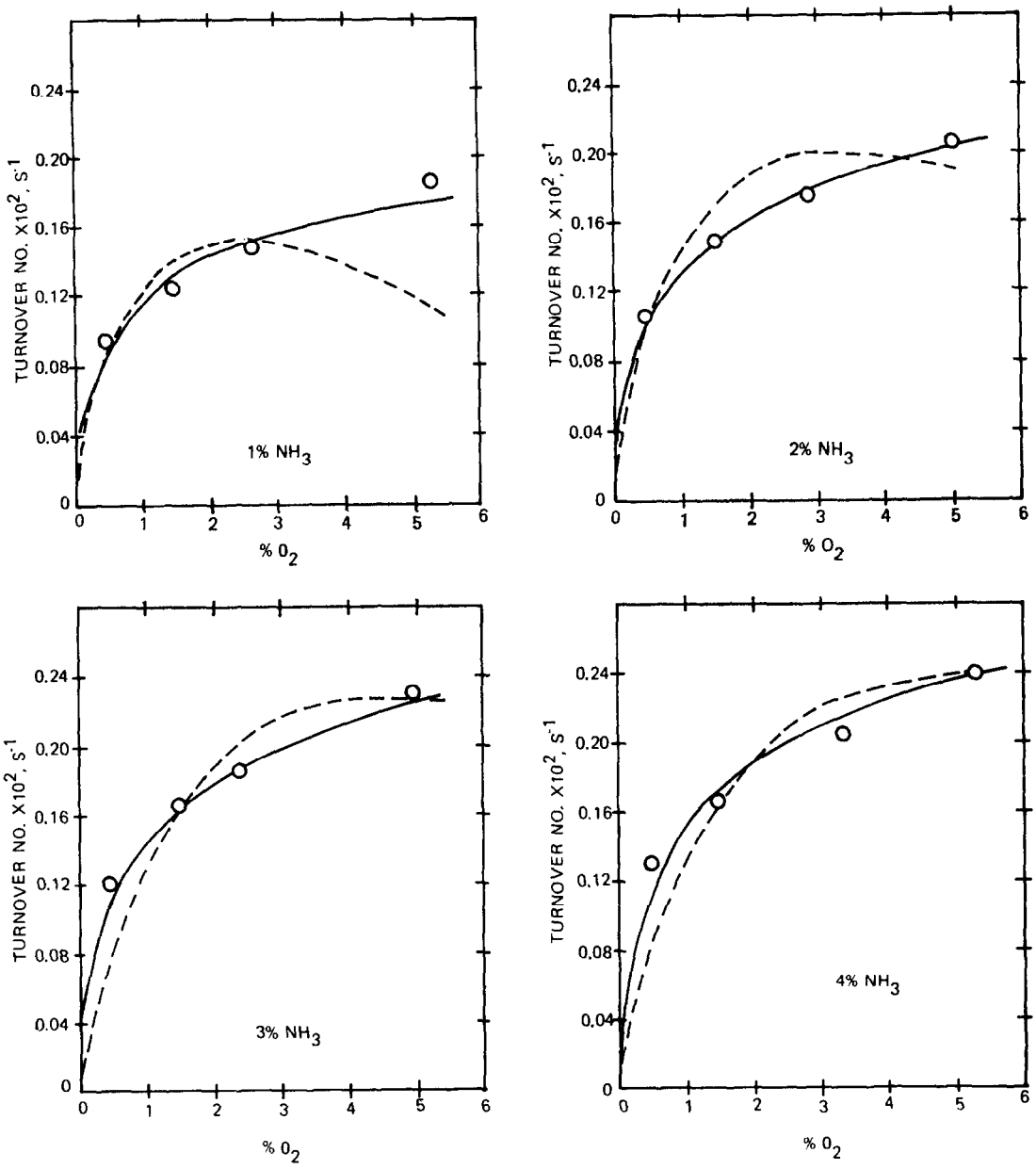

FIG. 6. Rate of ammonia oxidation over unsintered 1% Pt catalyst at 413°K and ability of kinetic models to represent data: (- -) predicted rate of reaction for model involving nondissociative adsorption; (—) predicted rate for model involving dissociative adsorption of both reactants [Eq. (1)].

Fig. 6 calculated from the model for nondissociative adsorption of both ammonia and oxygen. Model constants used in calculating the curve represent the best fit to the 30 point concentration-rate grid at 413°K. Both models involving the dissociative adsorption of oxygen represented the data satisfactorily. Table 6 gives calculated model parameters and percentage derivation for 95% confidence limits in the parameters. Table 6 further quantifies the crystallite size effect. The model for dissociative adsorption of both ammonia and oxygen represents the data better as indicated by the

TABLE 6
RATE MODEL PARAMETERS AND CONFIDENCE LIMITS ON PARAMETERS AT 413°K

		Model parameter and % deviation for 95% confidence limits			
		1% Unsintered Pt catalyst		1% Sintered Pt catalyst	
Rate model	Parameter	Value	% Deviation	Value	% Deviation
Dissociative O_2–	k_s	0.0174	6	0.098	6
nondissociative NH_3	K_{NH_3}	1950	28	2280	27
adsorption	K_{O_2}	890	12	3540	17
Dissociative O_2–	k_s	0.0225	4	0.142	4
dissociative NH_3	K_{NH_3}	751	11	764	10
adsorption	K_{O_2}	510	9	1370	13

significantly smaller confidence limits for the parameters of this model. The fit of this model to the data is shown by the solid curve in Fig. 6.

This model takes the form:

$$r_{NH_3} = \frac{k_s K_{NH_3}^{1/2} K_{O_2}^{1/2} P_{NH_3}^{1/2} P_{O_2}^{1/2}}{[1 + K_{NH_3}^{1/2} P_{NH_3}^{1/2} + K_{O_2}^{1/2} P_{O_2}^{1/2}]^2}. \quad (1)$$

DISCUSSION

Specific Catalytic Activity

The data indicate that NH_3–O_2 reaction occurs on the metal surface of the catalyst and that there is no significant contribution from the support. The products, nitrogen and nitrous oxide, are those expected for low-temperature oxidation of ammonia over platinum and many metal oxides (*21*, *28–34*). The only studies in variance with this are those of Nutt and Kapur (*35*), Fogel *et al.* (*36*), and Molinari *et al.* (*37*), all of whom operated at subatmospheric pressure and observed only nitric oxide and nitrogen as reaction products. The calculated Thiele modulus (*27*) for the highest rate observed at 433°K was about two orders of magnitude below the value for the onset of diffusional limitations, so that intrinsic kinetics were measured.

Extrapolation of the observed rate to zero time gives the rate of reaction on an undeactivated platinum surface and indicates a change in the specific catalytic activity of this surface with crystallite size. This appears to be a *primary crystallite size effect* (*38*) although we cannot absolutely rule out the possible occurrence of an initial, rapid crystallite size dependent deactivation, which could cause the observed difference in the initial specific catalytic activity.

The extent of deactivation is both temperature and crystallite size dependent and exhibits an activation energy of −14 and −18 ± 2 kcal/mole for the unsintered and sintered 1% Pt catalysts. Deactivation is believed due to the formation of a surface platinum oxide different from chemisorbed oxygen (*22*, *39*), and it is believed that the platinum surface below about 460°K is intrinsically different from that above 460°K with light-off. This is supported by the fact that the selectivity to nitrogen is about independent of temperature below 460°K; yet the effect of platinum crystallite size on selectivity for temperatures below 460°K is opposite that above 460°K (Tables 4 and 5).

The deactivation of the unsintered 1% Pt catalyst is about twice that of the sintered 1% Pt catalyst at all temperatures, and the smaller crystallite size 2.93% Pt catalyst is even more severely deactivated. This results in a further enhancement in the apparent *primary crystallite size effect* and is an example of a *secondary crystallite size effect* (*38*).

The Arrhenius activation energy for the initial rate (9 ± 2 kcal/mole) appears crystallite size independent and is considered a good estimate of the activation energy for

reaction over the undeactivated surface. The threefold higher values observed for steady-state conditions includes the effect of temperature on both surface reaction and extent of deactivation at steady-state. The sum of activation energy for initial rate and that for the extent of deactivation for each catalyst gives the activation energy observed at steady-state. The higher activation energy for the 15.5 nm crystallite catalyst at steady-state conditions is due to the greater dependency of the extent of deactivation on temperature for this catalyst.

The magnitude and direction of the crystallite size effect on specific catalytic activity observed here is consistent with that observed by Poltorak *et al.* (*3*, *4*, *17*) for oxidation reactions. The 14-fold decrease in steady-state specific catalytic activity for a dispersion of 0.52 and the indicated decrease with increasing dispersion indicate that the specific catalytic activity decrease may have approached the 100-fold decrease reported by Poltorak *et al.* (*3*, *4*) for ethanol oxidation if dispersions approaching theirs ($D > 0.95$) had been studied. They do not indicate whether they had catalyst deactivation during reaction, but they (*40*, *41*) report a crystallite size dependent activity change due to contact with air prior to reaction. We speculate that deactivation was present (*22*) and thus that their crystallite size effect was enhanced by it. The deactivation reported by Hanson *et al.* (*42*) for ethanol and by Leder and Butt (*43*) for hydrogen oxidation over supported platinum are undoubtedly due to deactivation of very small crystallites by oxygen. Kraft and Spindler (*44*) demonstrate an increased susceptibility of platinum to oxygen as crystallite size decreases. Susceptibility of very small platinum crystallites to oxygen alone as observed by Boudart *et al.* (*2*) in cyclopropane hydrogenation is related to but not the same as that observed here since our treatment of the catalyst under oxygen only caused no deactivation.

Selectivity

The data reveal a selectivity to nitrogen which is similar to that observed in oxide catalyst systems and which appears dependent on the concentration of active oxygen on the surface. We believe that the working surface is very much like that of an oxide catalyst, and we suggest that the selectivity of large and small platinum crystallites at temperature above and below 200°C can be explained on the basis of this concept.

The selectivity to nitrogen decreases for both crystallite size catalysts as the oxygen partial pressure is increased or as the ammonia partial pressure is decreased. This behavior is typical of oxide catalysts also where nitrogen and nitrous oxide are frequently the observed reaction products. Holbrook and Wise (*28*) observed that the selectivity to nitrogen decreased sharply as the oxygen partial pressure was increased in ammonia oxidation over cuprous oxide at 300°C. Doping metal oxides with monovalent ions results in increased amounts of extralattice oxygen, which consists of a tightly bound and a weakly bound form (*45-47*), and causes a marked increase in the rate of ammonia oxidation and a marked decrease in the selectivity to nitrogen (*29*, *30*). Krauss (*30*) and Johnstone, Hauvouras and Schowalter (*33*) concluded that this extralattice oxygen acts as active oxygen in the formation of nitrous oxide. BaO_2, which decomposes to BaO and oxygen at comparatively low temperatures, gives almost quantitative conversion of ammonia to nitrous oxide even in the absence of gas-phase oxygen (*31*).

In the case of platinum a reduction in the average surface concentration of readily available (active) oxygen with decreasing crystallite size is indicated by the increased selectivity to nitrogen, and the decreased specific activity.

A lower average surface concentration of readily available oxygen on smaller platinum crystallites is indicated by the observation of Wilson and Hall (*19*) that for oxygen the chemisorbed oxygen atom to surface platinum ratio increases from 0.5:1 to 1:1 as the platinum crystallite size increases from very small values. Theoretical calculations show that for palladium the chemisorption bond should be stronger for

very small crystallites than for larger ones (*48*), and that for small nickel crystallites the strength of adsorption of hydrogen increases as the coordination number of the surface nickel atom on which adsorption occurs decreases (*49*). This increasing trend in strength of adsorption bond should extend to oxygen chemisorption on plane, edge and corner atoms of platinum crystallites in that order.

The specific catalytic activity and the selectivity may be interpreted in terms of the effect of geometrical properties of the platinum crystallites on the surface composition and reactivity. Large crystallites (15.5 nm) for which over 98% of the surface platinum atoms are plane atoms (*3*, *4*) should exhibit high specific catalytic activity and low selectivity to nitrogen formation. Deactivation of such crystallites should alter the surface activity or decrease the total number of active sites available but would not necessarily alter the selectivity. For the platinum with a dispersion of 0.52 about 65% of the surface platinum atoms are plane atoms, 32% are edge atoms and 3% are corner atoms for perfect crystallites (*4*). If edge and corner atoms bind oxygen more strongly making it less readily available, the specific catalytic activity should decrease and the selectivity to nitrogen increase with decreasing crystallite size. Since the small crystallites contain two different types of surface platinum atoms in relatively equal quantities, deactivation which is more severe for one relative to the other will result in a selectivity shift.

Reaction Network and Kinetics

It is useful to invoke a reaction network for ammonia oxidation to explain the observed high N_2/N_2O ratio, its apparent dependence on the concentration of active oxygen, and the absence of nitric oxide as a reaction product. Nutt and Kapur (*35*) and Fogel *et al.* (*36*) working at low pressures observe nitric oxide as the product of the first reaction event which occurs on the catalyst surface. They find that both reacting species are adsorbed and find no evidence for the more complex reaction networks proposed by Bodenstein (*50*) or Andrussow (*51*). Tuszynski (*52*), Marczewska (*53*) and Zawadzki (*32*) provide additional evidence that nitric oxide is an intermediate product in ammonia oxidation under conditions more similar to ours. Nitric oxide once formed can react with ammonia on the surface (*54*). We propose the following reaction network:

$$NH_3 + 2S \rightleftarrows NH_{2(ad)} + H_{(ad)}, \quad (2)$$

$$O_2 + 2S \rightleftarrows 2O_{(ad)}, \quad (3)$$

$$NH_{2(ad)} + O_{(ad)} \rightarrow NH_2O_{(ad)} + S, \quad (4)$$

$$O_{(ad)} + NH_2O_{(ad)} \rightarrow NO_{(ad)} + H_2O + S, \quad (5)$$

$$NO_{(ad)} + NH_{2(ad)} \rightarrow [\text{Complex I}] \rightarrow N_2 + H_2O + 2S, \quad (6)$$

$$H_{(ad)} + NO_{(ad)} \rightarrow HNO_{(ad)} + S, \quad (7)$$

$$2HNO_{(ad)} \rightarrow [\text{Complex II}] \rightarrow N_2O + H_2O + 2S, \quad (8)$$

$$H_{(ad)} + O_{(ad)} \rightarrow OH_{(ad)} + S, \quad (9)$$

$$2\,OH_{(ad)} \rightarrow H_2O + O_{(ad)} + S. \quad (10)$$

Desorption of product species is implied, and surface intermediates follow the literature closely but are speculative. Reaction steps (2)–(5) follow generally Fogel *et al.* (*36*). Reaction steps (6)–(8) follow Otto, Shelef and Kummer (*54*) and represent only their major reaction paths. Under the partial conversion conditions of this study ammonia (*55*, *56*) and hydrogen (*57*) have been shown to react selectively with nitric oxide in the presence of molecular oxygen indicating that reaction steps (9) and (10) do not predominate. Observed product selectivity combined with material balance considerations show that about 75% of $H_{(ad)}$ formed goes to H_2O via reaction steps (9) and (10) and 25% goes via steps (7) and (8).

Dissociative adsorption of both reactants is indicated by the one-half order dependence of rate on reactant partial pressure demonstrated by the rate model which best fit the data [Eq. (1)]. This is particularly true for oxygen (Fig. 6). Pusateri, Katzer and Manogue (*26*) demonstrate one-half order dependence on ammonia partial pressure in the oxidation of ammonia by nitric oxide over supported platinum. They have also shown that a crystallite size effect is not present over supported platinum in the absence of molecular oxygen but is present

when molecular oxygen is added to the feed. Thus reaction steps (6)–(8) do not exhibit a crystallite size effect, and the effect in the NH_3–NO–O_2 system appears to enter earlier in the reaction network, probably reaction steps (4) or (5). If reaction step (4) or (5) is rate limiting either partially or completely and is demanding, the overall reaction should exhibit a crystallite size effect in both rate and selectivity.

A rate equation which is very similar to Eq. (1) in terms of dependence on gas-phase partial pressures in both the numerator and denominator can be derived from the proposed reaction network if reaction steps (5) and (9) are assumed rate determining with all earlier steps assumed in equilibrium, and if the amount of hydrogen consumed in reaction step (7) is neglected. The former assumption allows the selectivity data to be effectively explained by the proposed reaction network; the latter one is a reasonable approximation since the amount of nitrous oxide produced represents a small fraction of the total nitrogen and water formed by reaction steps (6) and (9), respectively, and it results in a marked simplification of the model equation derived. The fraction of surface covered by atomic hydrogen is obtained from a steady-state balance on $H_{(ad)}$. The derived rate expression was not fit to the data because of its complex denominator and its closeness in functional form to Eq. (1). (It would not have been possible to distinguish between the two equations.) The observed kinetics are consistent with the proposed reaction network with reaction step (5) rate limiting.

The kinetic model also indicates that changing oxygen interaction is the important factor in the crystallite size effect. The ammonia adsorption parameter does not change with crystallite size, but that for oxygen increases with crystallite size for both models, the increase being by a factor 2.7 for the best fit model (Table 6). This is consistent with the observation of increasing oxygen chemisorption stoichiometry with crystallite size of Wilson and Hall (*19*).

Selectivity to nitrogen should depend on the relative values of the rate constants for reaction steps (6), (7) and (9), and the relative surface concentrations of $NO_{(ad)}$, $NH_{2(ad)}$, $O_{(ad)}$, and $H_{(ad)}$. A higher specific catalytic activity for reaction step (5) should result in a higher relative concentration of $NO_{(ad)}$ and $H_{(ad)}$ and a lower concentration of $NH_{2(ad)}$. This should result in lower nitrogen production relative to nitrous oxide. For the above reaction network if the first three reaction steps are assumed at equilibrium, if the rate of disappearance of $NH_{2(ad)}$ and $H_{(ad)}$ are equated, and if a steady-state approximation is applied to the concentration of adsorbed NO, the resultant expression upon rearranging to give rate of nitrogen formation ($k_6\theta_{NO}\theta_{NH_2}$) divided by the rate of nitrous oxide formation ($1/2\ k_7\theta_H\theta_{NO}$) is:

$$\frac{r_{N_2}}{r_{N_2O}} = 1 + \frac{k_9\{k_6\theta_{NH_2} + k_7\theta_H\}\theta_{vs}}{k_7k_5K_4\theta_{NH_2}\theta_O} - \frac{k_6\theta_{NH_2}}{k_7\theta_H}. \tag{11}$$

Written in terms of gas-phase concentrations, Eq. (11) is very complex. Equation (11) predicts that the selectivity to nitrogen decreases as k_5 increases (higher specific activity with larger crystallites) and as the surface concentration of oxygen increases (higher partial pressure of oxygen). Equation (11) derived from the proposed reaction network, not only explains our selectivity behavior but is consistent with all of the selectivity behavior observed in ammonia oxidation by earlier workers (*28–31*, *33*).

The high selectivity to nitrogen under light-off conditions can also be related to surface concentrations of oxygen and hydrogen. Jones *et al.* (*57*) have shown that hydrogen reduces nitric oxide in the presence of molecular oxygen very selectively to about 473°K, and becomes less selective at higher temperatures. Under light-off conditions the concentration of oxygen on the surface is undoubtedly low, particularly at low P_{O_2}/P_{NH_3} ratios, and a larger fraction of this adsorbed oxygen reacts with $H_{(ad)}$ leading to a high selectivity to nitrogen. As the P_{O_2}/P_{NH_3} ratio increases, selectivity to nitrogen decreases according to an observed oxygen dependence slightly greater than

first order. The strong dependence on oxygen partial pressure is that of a relatively bare surface compared with the weak dependence of selectivity on oxygen partial pressure for the lower temperature, partial conversion conditions as would be predicted for a highly oxygen covered surface. These trends are also predicted by Eq. (11).

Conclusions

Ammonia oxidation over supported platinum exhibits a marked crystallite size effect and is a demanding reaction. Smaller crystallites have a lower specific catalytic activity than larger ones. This is opposite in trend to most cases of crystallite size effect under reducing conditions. This is in accord with the observation by Poltorak and co-workers (*3*, *4*, *17*) of crystallite size effects in other oxidation reactions and may indicate more generally that oxidation reactions are demanding. The initial specific catalytic activity was crystallite size dependent (a primary crystallite size effect), and the catalyst underwent deactivation to steady-state. This deactivation is considered due to a self-poisoning by oxygen with the deactivation of the smaller platinum crystallites being more pronounced than that of the larger ones leading to an enhancement of the crystallite size effect on specific catalytic activity (a secondary crystallite size effect). Activity and selectivity behavior are consistent with the proposed reaction network.

Acknowledgments

The financial support of this work by the National Science Foundation through Grant GK-34612X1 and an NDEA fellowship for J. J. O. are gratefully acknowledged. Electron micrographs of the catalysts taken by Dr. N. A. Neilsen of the DuPont Co. and helpful discussions by Dr. G. C. A. Schuit are gratefully acknowledged.

References

1. Aben, P. C., Plateeuw, J. C., and Stouthamer, B., *Proc. Int. Congr. Catal. 4th* **1**, 395 (1971).

2. Boudart, M., Aldag, A., Benson, J. E., Dougharty, N. A., and Harkins Given, C., *J. Catal.* **6**, 92 (1966).

3. Poltorak, O. M., Boronin, V. S., and Mitrofanova, A. N., *Proc. Int. Congr. Catal. 4th* **2**, 276 (1971).

4. Poltorak, O. M., and Boronin, V. S., *Zh. Fiz. Khim.* **40**, 1436 (1966).

5. Van Hardeveld, R., and Hartog, F., *Proc. Int. Congr. Catal. 4th* **2**, 295 (1971).

6. Cusumano, J. A., Dembinski, G. W., and Sinfelt, J. H., *J. Catal.* **5**, 471 (1966).

7. Kraft, M., and Spindler, H., *Proc. Int. Congr. Catal. 4th* **2**, 286 (1971).

8. Hughes, T. R., Houston, R. J., and Sieg, R. P., *Ind. Eng. Chem., Process Des. Develop.* **1**, 96 (1962).

9. Dautzenberg, F. M., and Platteeuw, J. C., *J. Catal.* **19**, 41 (1970).

10. Benson, J. E., and Boudart, M., *J. Catal.* **4**, 704 (1965).

11. Boudart, M., *in* "Advances in Catalysis" (D. D. Eley, H. Pines, P. B. Weisz, Eds.), Vol. 20, p. 153. Academic Press, New York, 1969.

12. Corolleur, C., Gault, F. G., Juttard, D., Maire, G., and Muller, J. M., *J. Catal.* **27**, 466 (1972).

13. Boreskov, G. K., and Chesalova, V. S., *Zh. Fiz. Khim.* **30**, 2560 (1956).

14. Boreskov, G. K., Slinko, M. G., and Chesalova, V. S., *Zh. Fiz. Khim.* **30**, 2787 (1956).

15. Andersen, H. C., Green, D. R., and Steele, D. R., *Ind. Eng. Chem.* **53**, 199 (1961).

16. Blurton, K. F., Greenberg, P., Oswin, H. G., and Rutt, D. R., *J. Electrochem. Soc. Electrochem. Sci. Technol.* **119**, 559 (1972).

17. Poltorak, O. M., and Boronin, V. S., *Zh. Fiz. Khim.* **39**, 1329 (1965).

18. Adamenkova, M. D., and Poltorak, O. M., *Zh. Fiz. Khim.* **37**, 741 (1963).

19. Wilson, G. R., and Hall, W. K., *J. Catal.* **17**, 190 (1970); **24**, 306 (1972).

20. Freel, J., *J. Catal.* **25**, 149 (1972).

21. DeLaney, J. D., and Manogue, W. H., *Proc. Int. Congr. Catal., 5th* (Paper No. 13) **1**, 237 (1973).

22. Ostermaier, J., Katzer, J. R., and Manogue, W. H., *J. Catal.*, submitted.

23. Joyner, G. L., "Scientific Glass Blowing" p. 257. Instruments Publ. Co., Pittsburgh, PA, 1949.

24. Adams, C. R., Benesi, H. A., Curtis, R. M., and Meisenhiemer, R. G., *J. Catal.* **1**, 336 (1962).

25. Klug, H. P., and Alexander, L. E., "X-Ray Diffraction Procedures," pp. 507–509. Wiley, New York, 1954.

26. Pusateri, R. J., Katzer, J. R., and Manogue, W. H., *AIChE J* **20**, 219 (1974).

27. Smith, J. M., "Chemical Engineering Kinet-

ics," Vol. 2, pp. 329–457. McGraw-Hill, New York, 1970.

28. HOLBROOK, L. L., AND WISE, H., *J. Catal.* **27,** 322 (1972).
29. GIORDANO, N., CAVATERRA, E., AND ZEMA, D., *J. Catal.* **5,** 325 (1966).
30. KRAUSS, W., *Z. Electrochem.* **53,** 320 (1949); **54,** 264 (1950).
31. KRAUSS, W., AND NEUHAUS, A., *Z. Phys. Chem. B* **50,** 323 (1941).
32. ZAWADZKI, J., *Discuss. Faraday Soc.* **8,** 140 (1950).
33. JOHNSTONE, H. F., HAUVOURAS, E. T., AND SCHOWALTER, W. R., *Ind. Eng. Chem.* **46,** 702 (1954).
34. SCHRIBER, T. J., AND PARRAVANO, G., *Chem. Eng. Sci.* **22,** 1067 (1967).
35. NUTT, C. W., AND KAPUR, S., *Nature (London)* **220,** 697 (1968); **224,** 169 (1969).
36. FOGEL, Y. M., NADYKTO, B. T., RYBALKO, V. F., SHVACHKO, V. I., AND KOROCHANSKYA, I. E., *Kinet. Katal.* **5,** 431 (1964).
37. MOLINARI, E., CRAMAROSSA, F., PULLO, A., AND TRIOLO, L., *J. Catal.* **4,** 341 (1965).
38. MANOGUE, W. H., AND KATZER, J. R., *J. Catal.* **32,** 166 (1974).
39. OSTERMAIER, J., PhD thesis, Dept. Chem. Eng., Univ. of Delaware, Newark, DE, 1973.
40. ADAMENKOVA, M. D., AND POLTORAK, O. M., *Zh. Fiz. Khim.* **37,** 741 (1963).
41. MITROFANOVA, A. H., BORONIN, V. S., AND POLTORAK, O. M., *Zh. Fiz. Khim.* **46,** 32 (1972).
42. HANSON, D. L., KATZER, J. R., GATES, B. C., SCHUIT, G. C. A., AND HARNSBERGER, H., *J. Catal.* **32,** 204 (1974).
43. LEDER, F., AND BUTT, J. B., *AIChE J.* **12,** 718 (1956).
44. KRAFT, M., AND SPINDLER, H., *Proc. Int. Congr. Catal., 4th* **2,** 286 (1971).
45. WINTER, E. R. S., *in* "Advances in Catalysis" (D. D. Eley, W. G. Frankenburg, V. L. Komarewsky and P. B. Weisz, Eds.), Vol. 10, p. 196. Academic Press, New York, 1958.
46. STONE, F. S., *in* "Advances in Catalysis" (D. D. Eley, P. W. Selwood and P. B. Weisz, Eds.), Vol. 13, p. 1. Academic Press, New York, 1962.
47. BIELANSKI, A., DEREN, J., HABER, J., AND STOCZYNSKI, J., *Trans. Faraday Soc.* **58,** 166 (1962).
48. BAETZOLD, R. C., *J. Chem. Phys.* **55,** 4363 (1971).
49. FASSAERT, D. J. M., VERBEEK, H., AND VAN DEN AVOIRD, A., *Surface Sci.* **29,** 501 (1972).
50. BODENSTEIN, M., *Z. Electrochem.* **41,** 517 (1941).
51. ANDRUSSOW, L., *Z. Angew. Chem.* **39,** 321 (1926).
52. TUSZYNSKI, K., *Rocz. Chem.* **23,** 397 (1949).
53. MARCZEWSKA, K., *Rocz. Chem.* **23,** 406 (1949).
54. OTTO, K., SHELEF, M., AND KUMMER, J. T., *J. Phys. Chem.* **74,** 2690 (1970).
55. SCHMIDT, K. H., AND SCHULTZ, V., *German Pat.* 1259298, Granted Jan. 25, 1968.
56. ANDERSEN, H. C., GREEN, W. J., AND STEELE, D. R., *Ind. Eng. Chem.* **53,** 199 (1961).
57. JONES, J. H., KUMMER, J. T., OTTO, K., SHELEF, M., AND WEAVER, E. E., *Environment Sci. Technol.* **5,** 790 (1971).